Molecular Therapy
Nucleic Acids
Original Article

Overexpression of Mutant FKRP Restores Functional Glycosylation and Improves Dystrophic Phenotype in FKRP Mutant Mice

Jason D. Tucker,[1] Pei J. Lu,[1] Xiao Xiao,[2] and Qi L. Lu[1]

[1]McColl-Lockwood Laboratory for Muscular Dystrophy Research, James G. Cannon Research Center, Carolinas Medical Center, Charlotte, NC 28203, USA; [2]Division of Molecular Pharmaceutics, Eshelman School of Pharmacy, University of North Carolina at Chapel Hill, Chapel Hill, NC 27599, USA

Autosomal recessive homozygous or compound heterozygous mutations in *FKRP* result in forms of muscular dystrophy-dystroglycanopathy varying in age of onset, clinical presentation, and disease progression, ranging from the severe Walker-Warburg, type A,5 (MDDGA5), muscle-eye-brain (MDDGB5) with or without cognitive deficit, to limb-girdle type 2I (MDDGC5). Phenotypic variation indicates degrees of functionality of individual FKRP mutation, which has been supported by the presence of residual expression of functionally glycosylated α-dystroglycan (DG) in muscles of both animal models and patients. However, direct evidence showing enhancement in glycosylation of α-DG by mutant FKRP is lacking. Using AAV9-mediated overexpression of mutant human FKRP bearing the P448L mutation (*mhFKRP-P448L*) associated with severe congenital muscular dystrophy (CMD), we demonstrate the restoration of functional glycosylation of α-DG and reduction in markers of disease progression. Expression of *mhFKRP-P448L* also corrects dystrophic phenotypes in the models of L276I mutation with mild disease phenotype and causes no obvious histological or biomarker alteration in *C57BL/6* normal mice. Our results confirm the existing function of mutant FKRP. The results also suggest that mutant FKRP could be an alternative approach for potential gene therapy should normal FKRP gene products be immunogenic.

INTRODUCTION

Dystroglycan (DG) is an essential component of the dystrophin-glycoprotein complex (DGC) required for the maintenance of muscle membrane stability by providing a physical linkage between the myofiber actin cytoskeleton and the extracellular matrix (ECM).[1–3] Originating from a single transcript, the DG protein is post-translationally cleaved into two subunits, α-DG and β-DG.[4] α-DG is extensively glycosylated with both *N*- and *O*-linked glycans and acts as a cellular receptor for laminin and other proteins, including agrin, perlecan, neurexin, and pikachurin, and as a receptor for old world arenavirus.[5–11] Interaction with ECM proteins depends upon *O*-linked manno-glycosylation in the centrally located mucin-like domain of α-DG.[12] Biochemical studies have established direct evidence for involvement of a number of the genes in glycosylation modifications of α-DG.[13–15] POMT1 and POMT2 catalyze the initial O-mannosylation of the protein. POMGnT2 (GTDC2) acts as a protein *O*-mannose β-1,4-N-acetylglucosaminyltransferase. Recently, FKRP and FKTN have been defined as ribitol 5-phosphate (Rbo5P) transferases with cytidine diphosphate ribitol (CDP-Rbo) as substrate, adding tandem ribo5P groups to core 3 of the *O*-mannosylated α-DG.[16–18] This structure is further extended with xylose by TMEM5 as xylosyltransferase and with GlcA by B4GAT1 as a xylose β1,4-glucuronyltransferase.[19–21] Lastly, LARGE acts as a bifunctional glycosyltransferase with both xylosyltransferase and glucuronyltransferase activity to produce repeating units of [–3-xylose– α1,3-glucuronic acid-β1–] and complete the following laminin-binding *O*-mannosyl glycan: [3GlcAβ1-3Xylα1]n-3GlcAβ1-4Xyl-Rbo5P1Rbo5P-3GalNAcβ1-3GlcNAcβ1-4(phospho-6)Manα1-α-DG.[19,22]

Numerous forms of muscular dystrophy arise from mutations in the genes associated with the post-translational glycosylation of α-DG. All forms of muscular dystrophy sharing reduced to absent functional glycosylation of α-DG are collectively termed the dystroglycanopathies. Dystroglycanopathies have been linked to autosomal-recessive mutations in at least 18 different genes, including those genes involved directly for the synthesis of the *O*-mannosyl glycan chain as described above. Mutations in the *FKRP* gene are the most common causes of dystroglycanopathy with a wide spectrum of clinical severity, ranging from severe congenital muscular dystrophies to limb-girdle muscular dystrophy type 2I (LGMD2I), varying in age of onset, clinical presentation, and disease progression with or without cognitive deficit.[19,22–24] The disease affects both cardiac and skeletal muscles with stress-related fiber damage followed by degeneration, inflammatory response, and regeneration.[19,22] The continuous loss of muscle fibers and diminishing capacity of regeneration eventually lead to the increase in fibrotic and fat tissues and loss of function.[19,22,25,26] However, clinical and therapeutic development

Received 17 November 2017; accepted 23 February 2018;
https://doi.org/10.1016/j.omtn.2018.02.008.

Correspondence: Qi L. Lu, McColl-Lockwood Laboratory for Muscular Dystrophy Research, James G. Cannon Research Center, Carolinas Medical Center, 1000 Blythe Boulevard, Charlotte, NC 28203, USA.
E-mail: qi.lu@carolinashealthcare.org

for the FKRP-related dystroglycanopathies during the last 15 years has been largely limited to the genetic diagnosis and analyses of genotype-phenotype correlation, with no effective therapy currently available. Gene therapy, especially adeno-associated virus (AAV)-mediated gene replacement, is currently the most promising therapeutic approach for the disease as a single gene loss-of-function mutation. Preclinical animal model tests with AAV9-mediated delivery of normal FKRP have shown significant therapeutic effect on both restoration of functionally glycosylated α-DG (F-α-DG) and improvement of muscle pathology.[27–29] However, clinical assessment remains to be conducted.

As previously reported, our group has created a number of mouse models representing *FKRP* mutations observed in human dystroglycanopathy patients.[15,30] These mice harbor the *FKRP* mutations, including *L276I* (*c.826C > T*), *P448L* (*c.1343C > T*), and *E310X* nonsense mutation. The *E310X* mutation is embryonic lethal in homozygous mice, whereas *L276I* mutation presents mild effect with later onset. The *FKRP P448L* mutant mice, with the removal of neomycin-resistant (Neo^r) cassette used for initial cloning and selection ($P448Lneo^-$) present severe muscular dystrophic phenotype without clear involvement in the CNS, a phenotype most like that reported in LGMD2I patients.[13,30] Studies of these mouse models demonstrate variable levels of F-α-DG, depending on the site of mutations and the levels of mutant FKRP expression.[30] Most interestingly, diseased muscles of both mouse models and human patients can contain a small proportion of fibers expressing up to normal levels of F-α-DG (revertant fibers).[31,32] Mechanisms for the restoration of F-α-DG in the revertant fibers are not clearly understood. One likely explanation is that the presence of F-α-DG indicates remaining function of the mutant FKRP protein, as it is generally understood that FKRP function is essential for F-α-DG.[33,34] Therefore, revertant fibers represent specific cellular conditions capable of compensating for the functional defect caused by mutations. Such cellular conditions are initially indicated by the revertant fibers associated with regeneration markers in diseased muscles of FKRP dystroglycanopathy. Restoration of F-α-DG has now been demonstrated in skeletal muscles during regeneration and in both skeletal and cardiac muscles in early stage of muscle development in P448L mutant mice.[33,34] However, direct evidence showing functionality of mutant FKRP with capacity to restore F-α-DG is still lacking. Confirmation of the functionality of mutant FKRP proteins and understanding the conditions that enable the fibers to restore the F-α-DG would be of value to several aspects of the diseases, for example, better explaining the variable disease phenotypes and, more importantly, developing novel therapies by possibly enhancing the expression of the endogenous mutant FKRP.

In the present study, we have examined the FKRP dystroglycanopathy mouse models, $P448Lneo^-$, *L276I*, and *C57BL/6* wild-type mice with AAV9-mediated overexpression of mutant human FKRP with P448L mutation (mhFKRP) to assess effects on expression of F-α-DG. The P448L mutation is associated with severe CMD phenotype and fails to support the production of F-α-DG in both skeletal and cardiac muscles, except for a few revertant fibers in the $P448Lneo^-$ mutant mice. In contrast to the Golgi localization of the normal FKRP, the mutant protein is predominantly mis-localized to the ER, which is a useful indicator for the nature of the protein and to be distinguished from wild-type FKRP.[33–37] We aimed to determine whether AAV-mediated P448L mutant FKRP overexpression is able to compensate for the same mutational defect in the $P448Lneo^-$ mutant mice to achieve functional glycosylation in muscles and, if so, whether the increased levels of F-α-DG is sufficient to alleviate disease severity. Overexpression of the mutant FKRP in wild-type mice would allow us to better determine detrimental effect to the muscular system without complication caused by the existing disease pathology in mutant mice. We demonstrate that overexpression of mutant FKRP restored expression of F-α-DG in the skeletal, diaphragm, and cardiac muscles in the $P448Lneo^-$ mutant and *L276I* mutant mice. Expression of the mhFKRP does not disturb the expression of F-α-DG in muscles of *C57BL/6* mice. These results confirm the capacity of mutant FKRP protein for F-α-DG, support efforts to modulate endogenous mutant FKRP as potential experimental therapy, and provide evidence for use of mutant FKRP as potential alternative for gene therapy should normal FKRP gene products prove immunogenic.

RESULTS

AAV9-mhFKRP-P448L Treatment Restores Expression of Functional O-Mannosylation of α-DG in FKRP $P448Lneo^-$ Mutant Mice

We first examined the transgene expression in different muscle tissues 1 month after the systemic delivery of 1×10^{13} or 5×10^{13} vg/kg of AAV9 vector expressing *mhFKRP* with the P448L mutation (*c.1343C > T*) driven by the cytomegalovirus (CMV) promoter. Immunohistochemistry with antibody to FKRP showed the majority of muscle fibers from heart, diaphragm and limb muscles treated with 5e13 vg/kg expressed detectable levels of FKRP, with the strongest signals in the cardiac muscle as reported previously (Figure 1A). Consistent with our previous report, the positive signals of the mhFKRP presented mainly as diffuse cytoplasmic staining without the specific pattern of Golgi localization, and this was further confirmed by confocal microscopic examination after double labeling for Golgi and the mhFKRP (Figure S1). The signal intensity varied considerably between muscles and within muscles. Only a small proportion of fibers with strong signal covering almost entire cross section areas were detected (less than 10%) in skeletal, with a higher proportion of the fibers (more than 15%) in cardiac muscles (Figure 1A). The signal was most pronounced at the periphery of myofibers in the skeletal muscle. The majority of fibers contained signals only as one to a few weak small cytoplasmic speckles, and the remaining proportion of fibers lacked detectable signal. This is especially notable in the diaphragm, where more than 50% of the fibers lacked convincing signal for the mhFKRP (Figure 1A). Considerably lower levels of mhFKRP were detected in the muscles treated with 1e13 vg/kg AAV9, and only small percentage (less than 1%) of fibers were detected with positive signals as one or a few small patches within the cytoplasm in skeletal muscles. Similar levels of mhFKRP

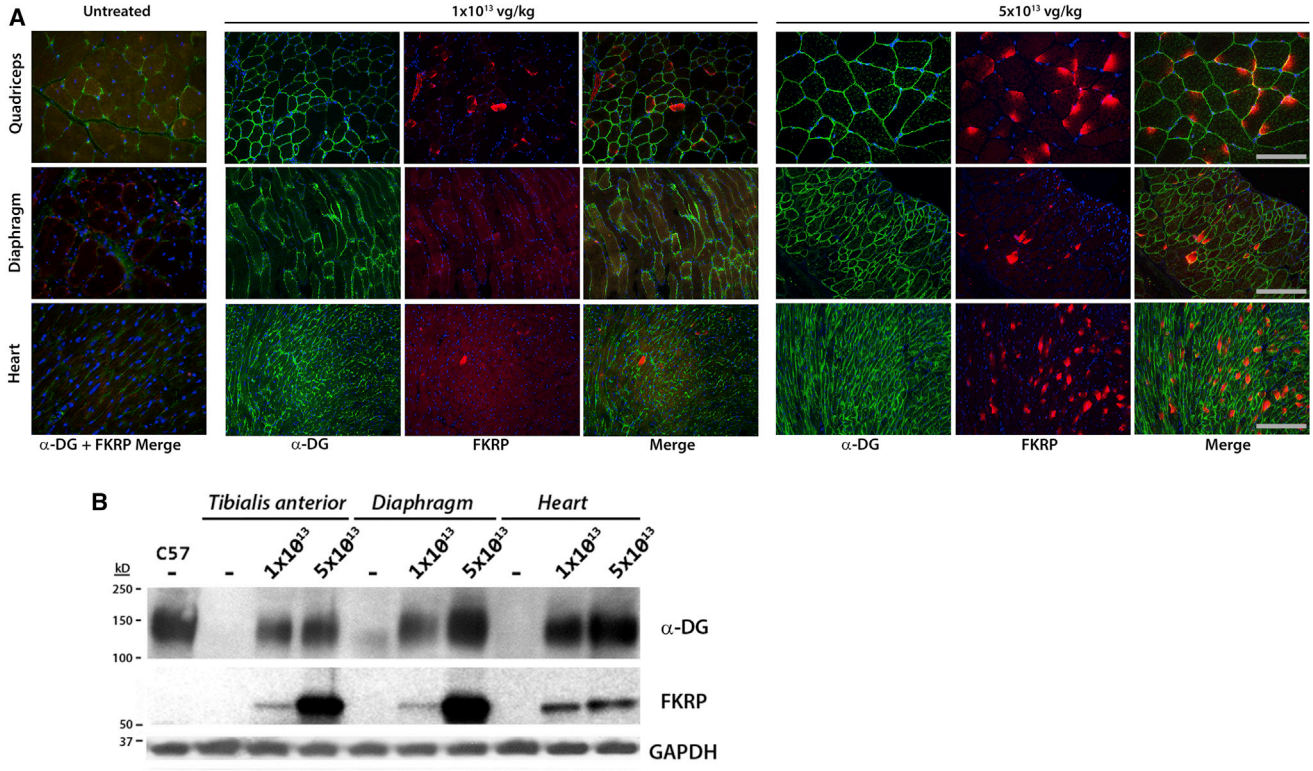

Figure 1. Restoration of Functional Glycosylation of α-DG in the *P448Lneo*⁻ Mouse after AAV9-mhFKRP Treatment

(A) Immunohistochemistry with antibodies (FKRP-Stem and IIH6) to FKRP and F-α-DG demonstrating dose-dependent levels of FKRP and F-α-DG signals in the majority of muscle fibers of the heart, diaphragm, and quadriceps treated with 1e13 and 5e13 vg/kg. Less than 1% of fibers with strong signal across section areas were detected in skeletal and cardiac muscles from mice treated with the lower doses of AAV9. The majority of the fibers in the diaphragm treated with both lower and higher doses of AAV9 lacks clear mhFKRP detection yet shows strong IIH6 detection. Untreated *P448Lneo*⁻ mice were used as controls (top left panel). The scale bars represent 200 μm. (B) Variable and dose-dependent levels of mhFKRP and F-α-DG expression were confirmed by western blot. A clear pattern of α-DG glycosylation can be observed in each tissue by both doses as compared to the untreated control to levels near that of the WT control (C57). TA, tibialis anterior muscle.

were also observed in a proportion of fibers of the cardiac muscle with signals as small weak spots, difficult to be distinguished from background (Figure 1A). The variable levels of expression were consistent with the results from western blot (Figure 1B).

The expression of F-α-DG in the P448L mutant muscles was first assessed by immunohistochemistry with the IIH6 antibody against the laminin-binding glycan epitope. In contrast to the heterogeneous levels of mhFKRP expression in the 5e13 vg/kg AAV9-treated mice, IIH6 signals were detected as fairly homogeneous membrane staining in the skeletal muscles, although a small proportion of fibers containing weak or no signal were also observed (Figure 1A). However, almost all cardiac muscle fibers showed strong membrane signals. The levels of mhFKRP and F-α-DG showed no clear spatial correlation, with no difference in IIH6 signal intensity between those fibers with strong mhFKRP signals covering almost the entire cytoplasm and those with only a few weak points for the mhFKRP. Large proportions of fibers lacking detectable mhFKRP expression also showed membrane IIH6 staining. Consistently, despite limited numbers of muscle fibers containing detectable mhFKRP in the mice treated with 1e13 vg/kg AAV9, more than 70% fibers expressed F-α-DG in the limb muscles. Similarly, more than 50% and 80% of the fibers in the diaphragm and cardiac muscle were F-α-DG positive, although the signals were weak and patchy at membranes of most fibers (Figure 1A). This is especially notable in the diaphragm, where more than 50% of the fibers lacked convincing signal for the mhFKRP (Figure 1A). The variable levels of expression were consistent with the results from western blot (Figure 1B). The fact that the majority of muscle fibers with clearly detectable F-α-DG are without clearly detectable mhFKRP is consistent with earlier reports with wild-type FKRP expression.[27,33,34,38]

AAV9-mhFKRP-P448L Treatment of *L276I* Mutant Mice Enhances Expression of F-α-DG

The *L276I* mutant mice 1 month after the systemic AAV9 treatment at 1e13 vg/kg dosage showed only minimal detectable levels of mhFKRP as one to a few trace points in a small proportion of the skeletal muscle fibers. A few sporadically distributed fibers with strong signals for mhFKRP were detected in the cardiac muscle (Figure 2). Expression of mhFKRP became clearly detectable in

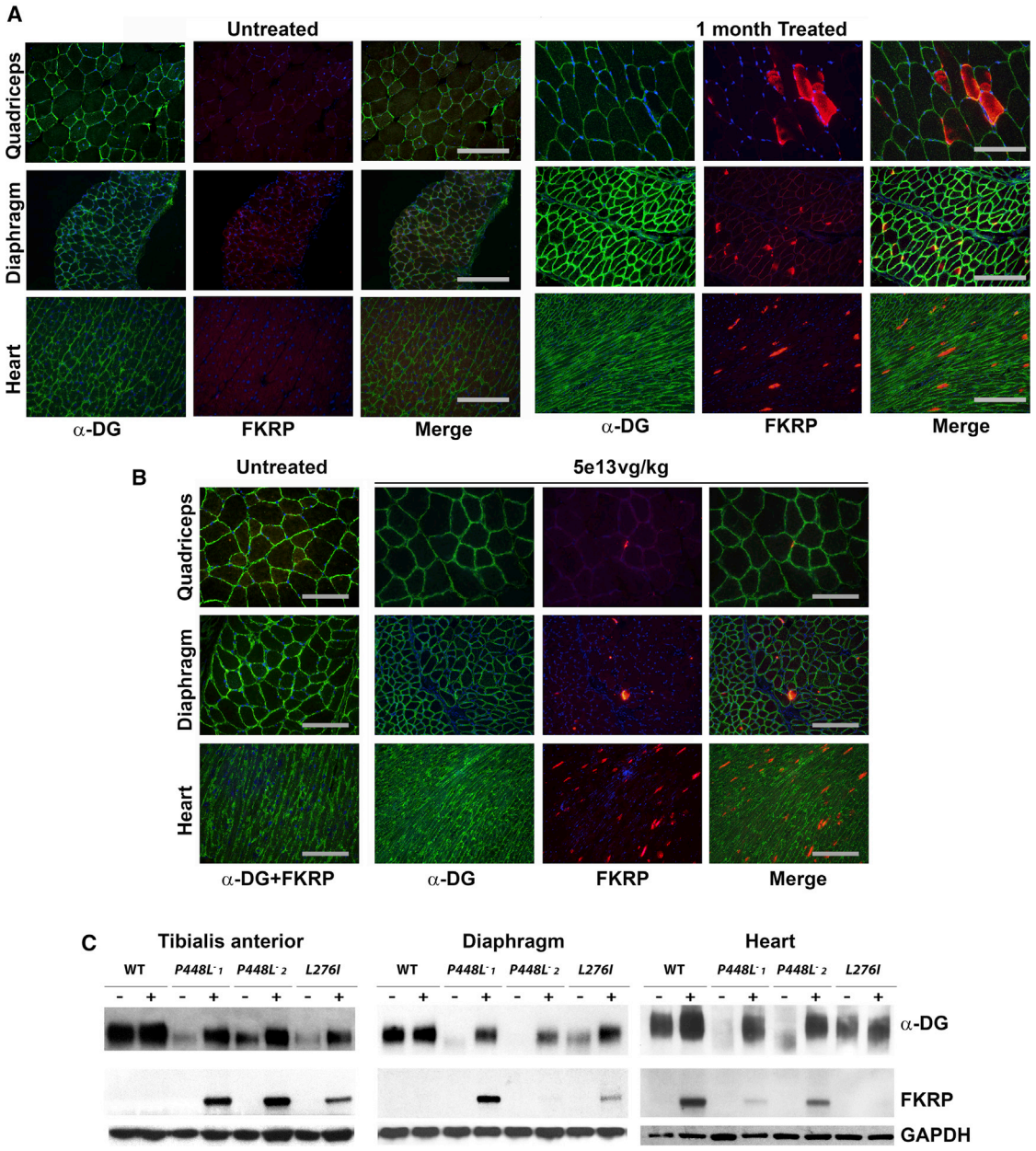

Figure 2. Expression of mhFKRP and F-α-DG (α-DG) in the Muscles of *L276I*, *P448Lneo*$^{-}$, and *C57BL/6* Mice (WT) with 5e13 vg/kg AAV9-mhFKRP Treatment

(A) Detection of mhFKRP and F-α-DG in the *L276I* mouse by immunohistochemistry. Expression of F-α-DG is clearly enhanced in all the muscles treated with AAV9-mhFKRP (middle column) when compared to the untreated (first column left). Mutant hFKRP forms patchy cytoplasmic red staining in a small proportion of the muscle fibers (second column right). The scale bars represent 200 μm. (B) Detection of mhFKRP and F-α-DG by immunohistochemistry in the WT mice. The mhFKRP expression did not affect the expression of detectable F-α-DG. The scale bars represent 200 μm. (C) Expression of both FKRP and F-α-DG in the 3 mouse models detected by western blot is shown. Lanes are marked as "−" untreated control samples and "+" AAV9-mhFKRP-treated samples 1 and 2 (from 2 treated mice).

the muscles with 5e13 vg/kg AAV9-*mhFKRP* treatment, but only less than 5% of the fibers showed strong cytoplasmic signals, and the majority of fibers remained without discernable signal. A similar pattern of the mhFKRP expression was observed in the cardiac muscles (Figure 2A). However, nearly all the muscle fibers from both heart and limb muscles and diaphragm displayed fairly uniform expression of F-α-DG, almost indistinguishable from the equivalent muscles of wild-type mice (Figure 2A). This is consistent, as the mice bearing the L276I mutation retain a moderate amount of F-α-DG in all muscles as we reported earlier and further confirmed in the control *L276I* mutant mice. The expression of both FKRP and F-α-DG was confirmed by western blot (Figure 2C).

Therefore, low levels of the mhFKRP, hardly detectable by immunohistochemistry and western blot in the majority of the muscles, appear sufficient to restore the F-α-DG to near normal levels in the homozygotes of the common L276I mutation.

AAV9-mhFKRP-P448L Treatment of *C57BL/6* Mice for 1 Month Results in mhFKRP Expression without Affecting Expression of F-α-DG

The pattern of mhFKRP expression in the muscles of the *C57BL/6* mice was similar to that observed in the muscles of *L276I* mutant mice. AAV9 treatment at 1e13 vg/kg showed only a few fibers with minimally detectable mhFKRP expression in all muscles. Mutant hFKRP was clearly detected by immunohistochemistry in the muscles with 5e13 vg/kg AAV9 treatment, but the positive fibers with strong cytoplasmic signal in the skeletal muscle were less than 1% and almost all other fibers contained no discernable signal. In the cardiac muscle, mhFKRP expression was easily detected in about 5% of fibers with strong signal, and the remaining fibers were either negative or contained weak signal as small stipples (Figure 2B). Expression of mhFKRP could not be clearly demonstrated in the skeletal muscles by western blots (Figure 2C). No significant difference in the expression of F-α-DG was detected between the AAV9-mhFKRP-treated and control mice as assayed by both immunohistochemistry and western blot (Figures 2B and 2C).

One-Month High-Dose AAV9-mhFKRP-P448L Treatment Improves Muscle Pathology of the *P448L* Mutant Mice

We examined the histology of muscles from *P448L* mutant, *L276I* mutant, and *C57BL/6* mice one month after the AAV9 treatment. No pathological changes were detected in the *C57BL/6* muscles (Figure 3A). The dystrophic pathology in the *L276I* muscle at the age of 10 weeks was minimal with only a few scattered degenerating fibers and a small proportion of centrally nucleated fibers (CNFs). No clear difference was observed between the AAV9 treated and the untreated control mice. In the *P448Lneo*$^{-}$ mutant mice, the low dose (1e13 vg/kg) of AAV9 treatment showed relatively limited effect on dystrophic pathology of the skeletal muscles, but a decrease in CNF was observed when compared to the untreated controls (Figure 3B). A reduction in fibrotic tissue in the diaphragm was also observed in the AAV9-*mhFKRP*-treated mice compared to the untreated group, with a higher degree of improvement associated with the higher dose AAV9 treatment as illustrated in Figures 3B and S2. At the age of 10 weeks, the cardiac muscle pathology of the *P448Lneo*$^{-}$ mutant mouse is limited to sporadic small areas of mononuclear cell infiltration and minor expansion of space between fibers. There was no clear difference in histology of the heart between the treated and untreated groups.

Six-Month Treatment of AAV9-mhFKRP-P448L Restores Expression of F-α-DG and Reduces Muscle Pathology in *FKRP P448Lneo*$^{-}$ Mice

To assess longer term effects of the mhFKRP overexpression, we further examined the *P448Lneo*$^{-}$ mutant mice 6 months after AAV9-mhFKRP-P448L treatment. The levels of mhFKRP expression decreased considerably compared to that observed at 1 month after treatment. Immunohistochemistry showed only a few sporadically distributed fibers with signals as one or two small points, most of which were located near the sarcolemma in skeletal muscles of the mice treated with 1e13 vg/kg AAV9 (Figure 4A). Signals for mhFKRP were not detected by western blot in all skeletal muscles and only minimally detectable in the cardiac muscle (Figure 4B). The expression of F-α-DG in the mice treated with 1e13 vg/kg AAV9, however, remained detectable in the majority of fibers of limb skeletal muscle and the diaphragm by immunohistochemistry, although positive membrane signals were weak and patchy (Figure 4A). Expression of F-α-DG was also easily detected in the cardiac muscle. However, the levels of F-α-DG were difficult to be clearly demonstrated by western blots (Figure 4B). Expression of mhFKRP was clearly detected at the sarcolemma in a small proportion of fibers of the skeletal muscle from the mice treated with 5e13 vg/kg as shown in Figure 4A. The expression was demonstrated in more than 30% of cardiac myocytes, with variable levels by immunohistochemistry and as clear bands by western blot. F-α-DG was detectable with the IIH6 antibody in the majority of fibers in skeletal muscles with relatively weak but homogeneous signals on membrane (Figure 4A). Similarly, weak signals were detected in the majority of cardiac muscle fibers. The expression of F-α-DG was clearly demonstrated in both skeletal and cardiac muscle by western blot (Figure 4B).

We also examined the effects of the mhFKRP expression on pathology of the *P448Lneo*$^{-}$ mice 6 months after initial treatment. Importantly, the treated mice showed a dramatic improvement in dystrophic markers in a dose-dependent manner, with TA and quadriceps having significant reduction in CNF even at the lower dose of 1×10^{13} vg/kg. Reduction in CNF, although less dramatic, was also observed in the treated diaphragm (Figures 4A and 5A). Fiber size distributions were not significantly changed at 1×10^{13} vg/kg dose. At the higher dosage of 5×10^{13} vg/kg AAV9, the numbers of CNFs and monocyte infiltration were significantly reduced, becoming almost comparable to wild-type (WT) control in the skeletal muscles. This improvement led to a normalized fiber size distribution in the diaphragm and limb muscles (Figure 5A), represented by the reduction in the coefficient of variance (CV) in fiber size of treated group as compared to untreated tissues, indicating a more homogeneous fiber morphology (Figure S3). Significant improvement in muscle pathology also included the reduction in fibrosis in skeletal muscle, particularly in the diaphragm by Masson's trichrome staining (Figure 5B). Pathology in cardiac muscle of the mutant mice remained limited at about 6 months with only small amounts of fibrotic tissue. Nevertheless, Masson's trichrome staining showed a considerable decrease in fibrotic areas of the treated mice when compared with the control mice (Figures 5B and 5C).

During the period after the AAV9 treatment, the mice showed no abnormal behavioral or physical indications (data not shown). H&E staining and serum enzyme tests showed normal histology and functions for the liver and kidney in all AAV9-treated mice (data not shown).

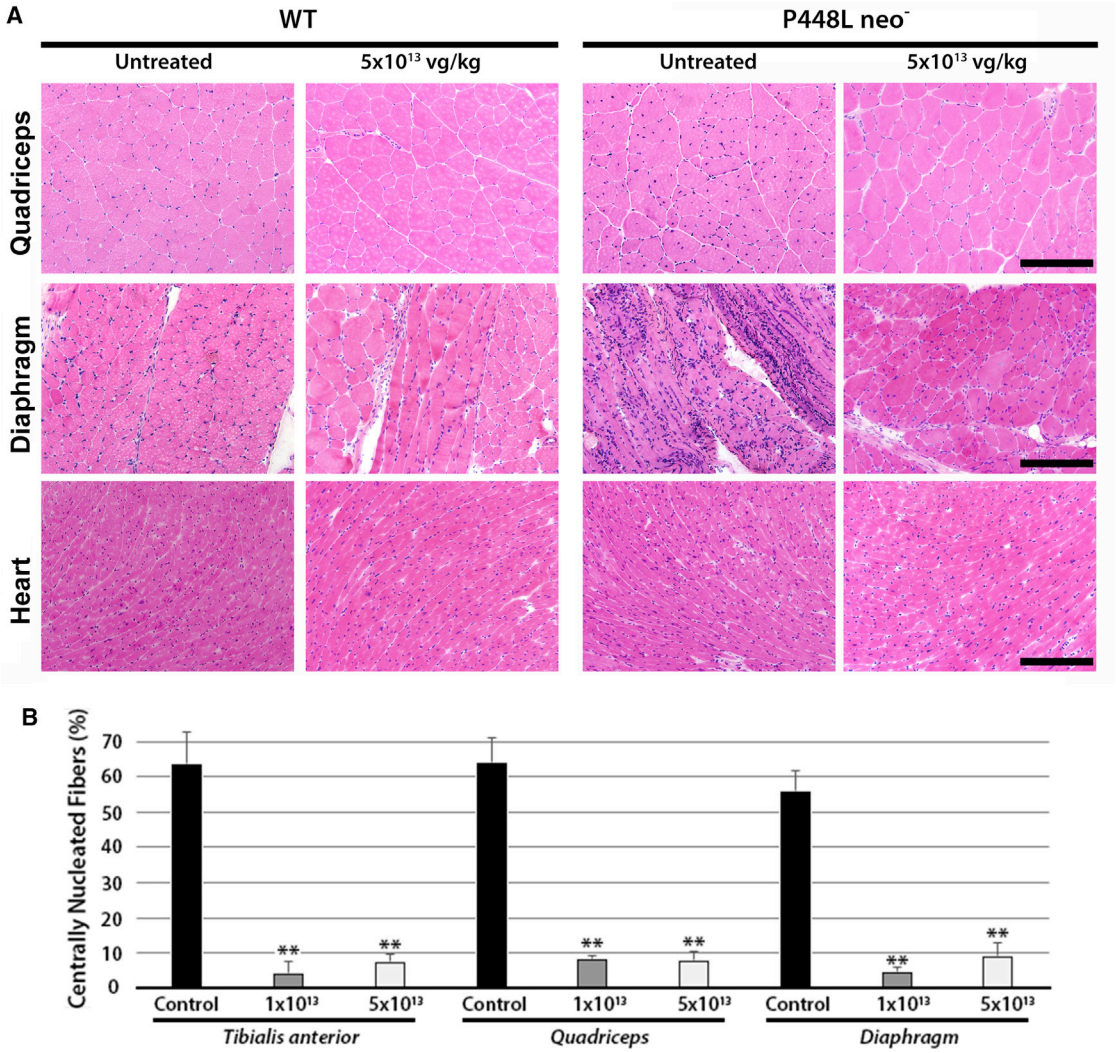

Figure 3. Morphological Analysis of Control and mhFKRP-Treated WT(*C57BL/6*) and *P448Lneo*$^{-}$ Mice

(A) H&E staining of WT and *P448Lneo*$^{-}$ mice 1 month after the treatment with 5 × 10^{13} vg/kg AAV9-mhFKRP-P448L. Treatment with mhFKRP reduced monocyte infiltration and central nucleated fibers in the mutant *P448L* mice. No clear changes are observed between treated and control WT groups. The scale bars represent 200 μm. (B) Centrally nucleated fibers in skeletal muscles of *P448Lneo*$^{-}$ mice are shown. Significant reduction is observed after both 1e13 and 5e13 vg/kg AAV9-mhFKRP treatment in the mutant mice. Error bars represent the SEM: **$p < 0.01$.

Mutant hFKRP-P448L Expression Has No Effect on Muscles of *C57BL/6* Mice Six Months after Treatment

Six months after the treatment with either dose of AAV9, the levels of mhFKRP expression became undetectable by immunohistochemistry and western blot in all skeletal muscles of the normal *C57BL/6* mice. However, signals of mhFKRP in the cardiac muscle were detected from the mice treated with the higher dose AAV9 by western blot but significantly less than that observed in the *P448Lneo*$^{-}$ mutant mice under the same dose treatment (Figure 4). The expression of F-α-DG of the treated mice remained largely indifferent from the control mice. There was no pathology in all muscles from the mice treated with both doses of the mhFKRP when compared to the normal *C57BL/6* mice (Figures 4A and 5B).

DISCUSSION

Loss of functional *O*-mannosylation of α-DG is the direct cause of muscle degeneration in dystroglycanopathies, including those with *FKRP* mutations. However, one intriguing biochemical feature in muscles bearing *FKRP* mutation is the presence of revertant fibers expressing F-α-DG.[15,30] Early studies in patient-derived diseased muscles identified the majority of revertant fibers as small in caliber and with central nucleation. Further, these fibers also express embryonic myosin, suggesting that they are associated with muscle regeneration.[32,33] We recently examined revertant fibers in two strains of *FKRP P448L* mutant mice (*c.1343C > T*; p.Pro448Leu), one with the neomycin-resistant (Neo^{r}) cassette (*P448Lneo*$^{+}$), and one with the cassette removed (*P448Lneo*$^{-}$).[15] The *P448Lneo*$^{+}$ mouse

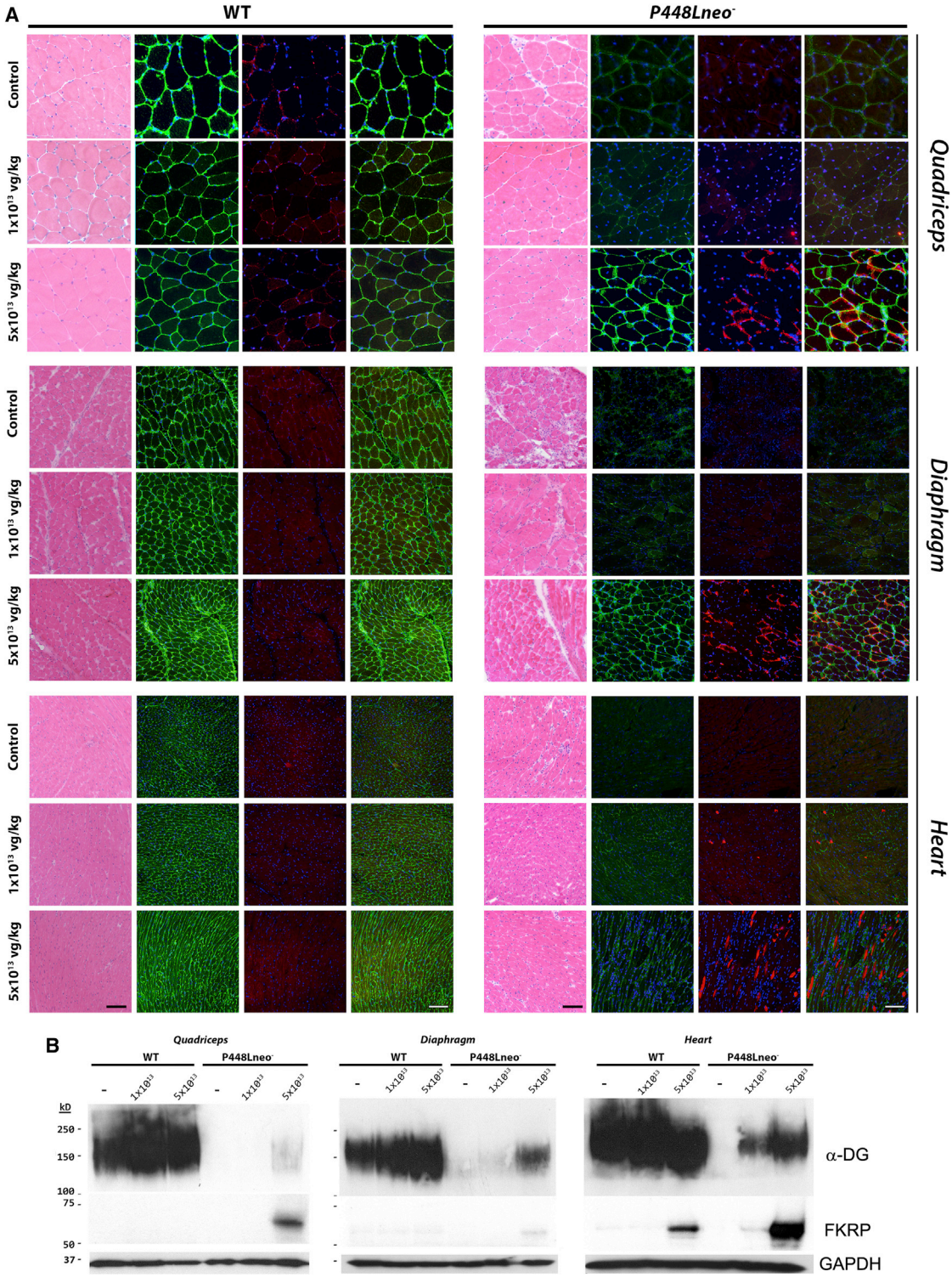

(legend on next page)

muscles express very low levels of the mutant FKRP and are associated with a more severe disease phenotype with CNS defects and embryonic or perinatal lethality. In comparison, the *P448Lneo*$^{-}$ mice have relatively higher levels of mutant FKRP with a milder disease phenotype without CNS involvement and breed normally.[30] Of these *FKRP P448L* mutant mice, the presence of revertant fibers is limited to the muscles from *P448Lneo*$^{-}$ mice and can be experimentally created by damage-induced muscle regeneration.[33] However, no clear expression of F-α-DG is demonstrated in the regenerating muscles of the *P448Lneo*$^{+}$ mice. A similar pattern in expression of F-α-DG is also observed in muscles of *P448Lneo*$^{-}$ homozygote neonates, but not *P448Lneo*$^{+}$ counterparts.[34] These results therefore suggest that *P448L* mutant FKRP retains certain levels of function and in the right circumstance is capable of restoring F-α-DG. Data from the current study now validate our notion that mutant FKRP, including P448L associated with clinically severe congenital disease phenotype,[13,24] retains sufficient capacity to restore normal levels of F-α-DG when overexpressed through AAV9-mediated gene delivery. One limitation in this study may be the use of the CMV promotor to drive the expression of mhFKRP, as the levels of transgene expression are likely higher than the same AAV construct if driven by another clinically preferred muscle-specific promoter. Therefore, the dose used to achieve therapeutic effect in this study will not be appropriate for dose estimation in the clinic. We also observed considerable decline in transgene expression by 6 months after the AAV9 treatment. The use of CMV promoter may be partly responsible.[39,40] Furthermore, the use of human mutant FKRP, which shares 94% sequence similarity to the mouse FKRP, could also elicit immune response that could lead to decline in expression as reported earlier for the human dystrophin expression in mouse.[41] The decline in transgene expression by 6 months may well explain the reduced therapeutic effect in some muscles with low viral dosage observed in this study.

The confirmation that FKRP mutations associated with severe disease phenotype could be sufficient to restore near normal levels of F-α-DG and rescue disease phenotype has several important implications to the mechanisms of the disease and further development of experimental therapies. One potential application is to use mutant FKRP for gene therapy. Current gene therapy strategies for the muscular dystrophies apply WT forms of a mutated gene to replace the lost function of that target gene. WT forms are generally considered preferable as therapeutic genes for achieving maximal functional restoration with minimal doses of transgene. However, variants of wild-type gene have been tested as transgene for treating muscular dystrophy, exemplified by the use of mini- and micro-dystrophin for Duchenne muscular dystrophy (DMD) due to size limitations in packaging by viral vectors, especially AAVs.[41] The use of truncated forms of dystrophins is initially rationalized from the observation that dystrophin with in-frame deletion mutations can be associated with mild Becker muscular dystrophy (BMD).[42] The mini- and micro-dystrophins therefore can be considered as mutant forms of dystrophin with reduced function, and their use for gene therapy has so far been largely successful in animal model studies. Thus, application of a mutant FKRP with reduced function for gene therapy utilizes the same principle but addresses the potential immune response of recipient to the presence of non-natural amino acid sequences expressed by a transgene. Currently, there is no clear means to determine preclinically whether a transprotein with limited sequences difference from the wild-type protein could elicit immune response and diminish the transgene expression in clinics. Animal model studies with transgene containing neo-sequences have largely reported minimal immune response to transgene products, as exemplified by the use of mini- and micro-dystrophin gene therapy for DMD. However, when human dystrophin is expressed in mice, immune response to human dystrophin is detectable.[41] Furthermore, an early clinical trial with a truncated dystrophin reports cytotoxic T cell response, which is associated with unexpected low levels of transgene expression, although the exact mechanism for the immune response remains unclear.[43,44] Gene therapy expressing a protein variant with only 3 amino acid difference from the natural protein has also reported immune response to the trans-protein in clinical trials.[45] Clearly, identical protein sequence as expressed by patients is ideal, and the common *L276I* mutation could be one of choice, as homozygote mutations are almost invariably associated with mild LGMD2I with reduced rather than complete loss of F-α-DG. Furthermore, most compound heterozygotes also contain *L276I* mutation, enabling this mutant transgene to be applied to more than 90% of the cases with FKRP mutations without introducing new sequence variants to the patient. However, the use of mutant FKRP as transgene for therapy is not currently warranted, as the probability of a single amino acid difference between the wild-type FKRP and the mutant FKRPs to elicit immune response is considered low. Our findings nevertheless offer an alternative if required.

One concern associated with gene therapy is the potential side effects of overexpression of a trans-protein. Recently, Gicquel et al.[46] described a dose-dependent reduction of F-α-DG in muscles of wild-type and an *L276I* mutant mouse model after local AAV2/9-FKRP intramuscular injection. Associated with the reduction of F-α-DG in the high-dose AAV2/9-FKRP-injected muscle is significant inflammation and muscle damage, as demonstrated by both

Figure 4. H&E Staining and Immunohistochemical Detection of F-α-DG and mhFKRP Expression in *C57BL/6* (WT) and *P448Lneo*$^{-}$ Mice Six Months after AAV9-mhFKRP Treatment

(A) H&E staining, left panel. Detection of mhFKRP (red) with FKRP-Stem antibody and F-α-DG (green) with IIH6 antibody in untreated, 1e13 vg/kg, or 5e13 vg/kg treated quadriceps, diaphragm, and heart tissues is shown. Dose-dependent restoration of F-α-DG was observed in *P448Lneo*$^{-}$ tissues. Mutant hFKRP was not clearly detected in the treated WT mice, and no change was observed in the IIH6 signal between the treated and control WT mice. The scale bars represent 100 μm. (B) Detection of mhFKRP and F-α-DG in quadriceps, diaphragm, and heart by western blot is shown. Enhanced F-α-DG was detected in the mhFKRP-treated *P448Lneo*$^{-}$ mice. Mutant hFKRP was detected only in the heart of higher dose AAV9-mhFKRP-treated WT mice.

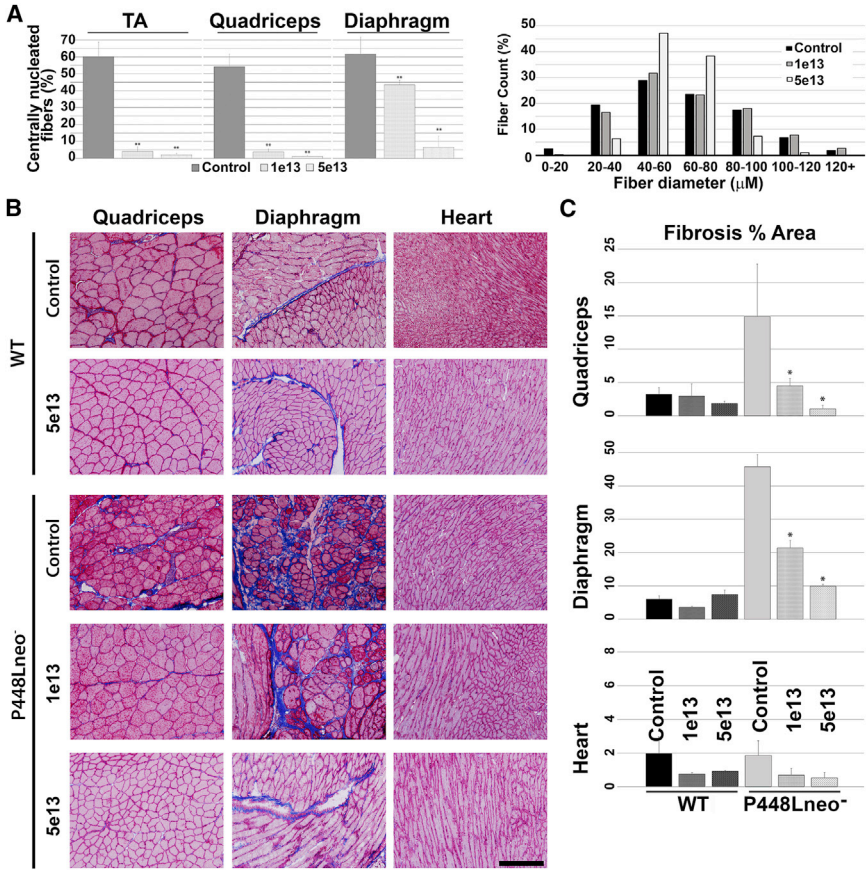

Figure 5. Histological and Morphological Analysis of Control and mhFKRP-Treated WT and *P448Lneo*$^{-}$ Mice Six Months after mhFKRP Administration

(A) Morphometrically measured benefit of mhFKRP expression to *P448Lneo*$^{-}$ mice with significantly reduced centrally nucleated fibers in the TA, quadriceps, and diaphragm, as well as normalization in fiber size distribution pattern. (B) Masson's-trichrome-stained tissues of untreated and treated *C57BL/6* (WT) and *P448Lneo*$^{-}$ mice are shown. The scale bars represent 200 μm. (C) Quantification of fibrosis indicated by Masson's trichrome staining is shown. Significant reduction in fibrosis was observed in the skeletal muscles of the treated *P448Lneo*$^{-}$ mouse. No significant change was observed between the treated and control WT mice, including cardiac tissues from all mice. Error bars represent the SEM.

histology and infiltration markers. Although the authors reported that injection of an AAV2/9 vector not coding for any protein did not affect glycosylation of α-DG, the local immuno-stimulatory effects and pathology of the control AAV-treated muscles are not described. It is therefore difficult to conclude whether the reported local effects of the AAV treatment is the result of FKRP overexpression or a local injection-related event. At the same time, the authors report significant therapeutic effect of the *FKRP* gene therapy in *L276I* mutant mice without any toxicity via systemic administration. Effective gene therapy for muscular dystrophy will certainly rely on systemic restoration of target gene expression. Our earlier studies of systemic delivery of AAV9 with doses higher than that reported by Gicquel et al. also show no identifiable side effect.[27,29,38] In the current study, we demonstrate that overexpression of *P448L* mutant FKRP systemically restores up to near normal levels of F-α-DG in 2 strains of mutant FKRP mice with improved dystrophic phenotype and results in no histological evidence of damage to muscles in both the *C57BL/6* and *L276I* mutant mice. The levels of mutant FKRP expression are very high within 1 month, likely due to the use of the CMV promotor, in a proportion of skeletal and cardiac muscle fibers. These fibers remain histologically normal, with clear membrane signals for F-α-DG. Our earlier study with normal FKRP as the transgene produced a similar result in the same FKRP mutant model.[27] The collective data therefore suggest that overexpression of FKRP up to the levels that can achieve restoration of normal levels of F-α-DG via systemic delivery of the transgene is not associated with detrimental effect within the time frame examined.

In summary, our study confirms the notion that FKRP mutations, even those associated with severe disease phenotypes, retain partial function. The fact that no side effects are detected in association with the overexpression of the mutant FKRP in both normal and mutant mice supports the potential use of mutant FKRP as alternative for gene therapy to restore functional glycosylation of α-dystroglycan.

MATERIALS AND METHODS

AAV Vector Construction and Production

The mutant FKRP construct ΔC1343T (P448L) was generated by PCR-directed mutagenesis using primers containing the mutant nucleotide underlined: P448L-MF1-mhFKRP, 5′-CTTCCTGCAG CTGCTGGTGC-3′; and P448L-MR1-mhFKRP, 5′-GCACCAGC AGCTGCAGGAAG-3′ (Stratagene), as described previously.[35] The full 1,488-bp coding sequence of mhFKRP-P448L was sub-cloned into AsiS1 site of the pAV-FH vector under the control of the CMV promoter. AAV9 viral stocks with the recombinant AAV vector were produced according to the three-plasmid co-transfection method by ViGene Biosciences, Rockville, MD.

Mice

AAV9 vector expressing the human FKRP with the *P448L* mutation (*c.1343C > T*; *mhFKRP*) was administered intravenously in homozygous *P448Lneo*$^{-}$, *L276I*, and *WT* (*C57BL/6 /Bl6*) mice. The mice were treated once at 6 weeks of age with the doses of 1×10^{13} vg/kg and 5×10^{13} vg/kg body weight in sterile saline suspension (referred to as 1e10 and 5e10 groups) and assessed 1 month and 6 months after

treatment for muscle histology and immunohistochemical features. This study was carried out in accordance with the recommendation in The Guide for the Care and Use of Laboratory Animals of the NIH, and the protocol was reviewed and approved by the Institutional Animal Care and Use Committee (IACUC) Carolinas Medical Center (10-13-08A). A minimum of three mice ($n \geq 3$) were used for each experimental group in all experiments, with six mice in each experimental group except the six-month control C57BL/6, which had 4 mice.

Immunohistochemical and Western Blot Analysis

Tissues collected were snap frozen in liquid-nitrogen-chilled isopentane. Cross sections of 6 μm thickness were cut from the frozen tissues and stained with H&E, Masson's trichrome, or immunofluorescent protocols. Immunohistochemical staining of F-α-DG was performed on serial sections fixed with ice-cold 50% ethanol and 50% acetic acid for 1 min and blocked with 8% BSA in PBS for 1 hr. Primary antibody against α-DG (IIH6C4; Millipore, Temecula, CA, USA) in 1% BSA at 1:500 dilutions was incubated overnight at 4°C. For FKRP-Stem 829 (FKRP-Stem) immunostaining, sections were incubated with the primary antibody[36,37] (a gift from Dr. Derek Blake), washed three times for 10 min with PBS, and finally incubated with Alexa-488-conjugated anti-mouse or Alexa-Fluor-594-conjugated anti-rabbit secondary antibodies (Life Technologies, Carlsbad, CA, USA) at 1:500 dilution. For Golgi marker GM-130 (GM-130) immunostaining, sections were incubated with the primary antibody (BD Biosciences, San Jose, CA, USA), washed three times for 10 min with PBS, and finally incubated with Alexa-488-conjugated anti-mouse or Alexa-Fluor-594-conjugated anti-rabbit secondary antibodies (Life Technologies, Carlsbad, CA, USA) at 1:500 dilution. Immunostaining controls consisted of matched sections stained with secondary antibody only as negative control. Positive fibers in detection of α-DG or mhFKRP were calculated from counts of ≥1,000 total number of fibers in triplicate tissue cross sections and expressed as percent (positive fibers/total fibers) × 100.

H&E-stained sections and immunofluorescence were visualized using an Olympus BX51 fluorescent microscope (Opelco, Dulles, VA, USA). Images were captured using an Olympus DP70 CCD camera system (Opelco, Dulles, VA, USA) at standard gain and matched exposure times.

For western blot analysis, tissue sections (10 μm) were lysed in Triton lysis buffer containing 1% Triton X-100, 50 mM Tris (pH 8.0), 150 mM NaCl, 1 mM EDTA, 0.1% SDS, and a Protease Inhibitor Cocktail (Sigma-Aldrich, St. Louis, MO, USA). The protein concentration of cleared lysates was determined using the Bradford method (Bio-Rad, Hercules, CA, USA). Total protein 50 μg each, unless specified otherwise, was analyzed on 4%–15% Criterion Precast Gel (Bio-Rad, Hercules, CA, USA) and transferred onto supported nitrocellulose membrane (Bio-Rad, Hercules, CA, USA).

For western blot α-DG detection, membranes were blocked after gel transfer with 3% milk in PBS for 2 hr at room temperature before addition of primary antibody. The immunoglobulin M (IgM) anti-α-dystroglycan primary antibody IIH6C4 (Millipore, Temecula, CA, USA) was used at dilution 1:2,000 in fresh blocking buffer and incubated for 1 hr at room temperature prior to overnight incubation at 4°C. Membranes were washed briefly several times with ddH2O. Secondary antibody, horseradish peroxidase (HRP)-goat anti-mouse IgM (Pierce, Rockford, IL, USA) at a dilution of 1:3,000 was incubated for 2 hr at room temperature, washed with ddH2O, and followed with a final wash with PBS+0.05% Tween 20 for 5 min. Resultant blot was briefly saturated with Western-Lightning Plus ECL (Perkin-Elmer, Wellesley MA, USA) before exposure and developing of GeneMate auto-radiographic film (VWR, Radnor, PA, USA).

For western blot FKRP detection, membranes were blocked after gel transfer with 5% milk in TBS+0.05% Tween 20 for 2 hr at room temperature. Primary antibody used was affinity-purified polyclonal rabbit anti-FKRP (C-terminal; sequence NPEYPNPALLSLTGG) produced in our laboratory applied at a dilution of 1:500 in fresh blocking buffer and incubated overnight at 4°C. Membranes were washed with 1× TBS-T to remove unbound primary antibody twice for 10 min followed by incubation with horseradish-peroxidase-conjugated goat anti-rabbit IgG (Bio-Rad), washed, and briefly saturated with Western-Lightning Plus ECL (Perkin-Elmer, Wellesley, MA, USA) before exposure and developing of auto-radiographic film (GeneMate). For loading controls, α-actin, or anti-α-glyceraldehyde 3-phosphate dehydrogenase GAPDH, membranes were blocked after gel transfer with 5% milk in TBS+0.05% Tween 20 for 2 hr at room temperature. Primary antibodies used were rabbit polyclonal anti-α-actin (Sigma-Aldrich, St. Louis, MO) and GAPDH (Thermo Fisher Scientific, Rockford, IL, USA) applied at a dilution of 1:500 and 1:3,000, respectively, in fresh blocking buffer and incubated overnight at 4°C. Membranes were washed twice with 1× TBS-T to remove unbound primary antibody for 10 min followed by incubation with horseradish-peroxidase-conjugated goat anti-rabbit IgG (Bio-Rad), washed, and briefly saturated with Western-Lightning Plus enhanced chemiluminescence (Perkin-Elmer, Wellesley, MA, USA) before exposure and developing of auto-radiographic film (GeneMate).

For blot densitometry measurements, films generated from western blots were scanned to image files and used for densitometric measurement with ImageJ. All measures were normalized to background and internal references or controls. For densitometric comparisons, regions of interest (ROIs) of equal dimensions were used for treatment and control groups and were normalized by local background. All measures were performed in triplicate using ImageJ v1.51i.[47]

Histopathology and Morphological Analysis

Tissue photomicrographs captured at standard magnification with calibrated scale bars (Olympus America, Center Valley, PA, USA) were used for measures including counts of CNFs and fiber size distributions using ImageJ (v1.5i). A minimum of 4 H&E-stained tissue sections were used where tissue cross sections represented all areas of assessed tissues, with a minimum of 3,000 ROIs for size analysis, or individual fibers counts for assessing centrally nucleated fiber counts. Sections from snap-frozen tissues stained

with modified Masson's trichrome protocol were captured as digital images as described previously and assessed for collagen using color thresholds to calculate content as a percentage by (ROI area/total area) × 100.

Statistical Analysis

Simple comparisons were performed using Student's t test, where two-tailed p value ≤ 0.05 was considered significant. Power analysis was used to ensure an appropriate number of samples were included in all measures, with n selected in comparisons to be equivalent to larger sample size determined through power analysis. Statistical significance where noted in figures is used as follows: *$p < 0.05$; **$p < 0.01$; and ***$p < 0.001$.

SUPPLEMENTAL INFORMATION

Supplemental Information includes three figures and can be found with this article online at https://doi.org/10.1016/j.omtn.2018.02.008.

AUTHOR CONTRIBUTIONS

J.D.T. and P.J.L. conducted experimental procedures. J.D.T. and Q.L.L. wrote the paper. J.D.T. and Q.L.L. designed experiments, with expert advice from X.X. and P.J.L.

CONFLICTS OF INTEREST

The authors of this work declare no conflict of interest.

ACKNOWLEDGMENTS

This work was supported by the Carolinas Muscular Dystrophy Research Endowment through the Carolinas Healthcare Foundation. The authors thank the staff of the Comparative Medicine Facility and Research Histology Core and of the James G. Cannon Research Center at Carolinas Medical Center. We also wish to thank Prof. Derek Blake (Cardiff University, Cardiff, Wales, UK) for the generous gift of the FKRP antibody.

REFERENCES

1. Ervasti, J.M., and Campbell, K.P. (1991). Membrane organization of the dystrophin-glycoprotein complex. Cell *66*, 1121–1131.
2. Ervasti, J.M., and Campbell, K.P. (1993). A role for the dystrophin-glycoprotein complex as a transmembrane linker between laminin and actin. J. Cell Biol. *122*, 809–823.
3. Kanagawa, M., and Toda, T. (2006). The genetic and molecular basis of muscular dystrophy: roles of cell-matrix linkage in the pathogenesis. J. Hum. Genet. *51*, 915–926.
4. Ibraghimov-Beskrovnaya, O., Ervasti, J.M., Leveille, C.J., Slaughter, C.A., Sernett, S.W., and Campbell, K.P. (1992). Primary structure of dystrophin-associated glycoproteins linking dystrophin to the extracellular matrix. Nature *355*, 696–702.
5. Campanelli, J.T., Roberds, S.L., Campbell, K.P., and Scheller, R.H. (1994). A role for dystrophin-associated glycoproteins and utrophin in agrin-induced AChR clustering. Cell *77*, 663–674.
6. Gee, S.H., Montanaro, F., Lindenbaum, M.H., and Carbonetto, S. (1994). Dystroglycan-alpha, a dystrophin-associated glycoprotein, is a functional agrin receptor. Cell *77*, 675–686.
7. Brown, S.C., Fassati, A., Popplewell, L., Page, A.M., Henry, M.D., Campbell, K.P., and Dickson, G. (1999). Dystrophic phenotype induced in vitro by antibody blockade of muscle alpha-dystroglycan-laminin interaction. J. Cell Sci. *112*, 209–216.
8. Talts, J.F., Andac, Z., Göhring, W., Brancaccio, A., and Timpl, R. (1999). Binding of the G domains of laminin alpha1 and alpha2 chains and perlecan to heparin, sulfatides, alpha-dystroglycan and several extracellular matrix proteins. EMBO J. *18*, 863–870.
9. Sugita, S., Saito, F., Tang, J., Satz, J., Campbell, K., and Südhof, T.C. (2001). A stoichiometric complex of neurexins and dystroglycan in brain. J. Cell Biol. *154*, 435–445.
10. Sato, S., Omori, Y., Katoh, K., Kondo, M., Kanagawa, M., Miyata, K., Funabiki, K., Koyasu, T., Kajimura, N., Miyoshi, T., et al. (2008). Pikachurin, a dystroglycan ligand, is essential for photoreceptor ribbon synapse formation. Nat. Neurosci. *11*, 923–931.
11. Cao, W., Henry, M.D., Borrow, P., Yamada, H., Elder, J.H., Ravkov, E.V., Nichol, S.T., Compans, R.W., Campbell, K.P., and Oldstone, M.B. (1998). Identification of alpha-dystroglycan as a receptor for lymphocytic choriomeningitis virus and Lassa fever virus. Science *282*, 2079–2081.
12. Yoshida-Moriguchi, T., and Campbell, K.P. (2015). Matriglycan: a novel polysaccharide that links dystroglycan to the basement membrane. Glycobiology *25*, 702–713.
13. Brockington, M., Yuva, Y., Prandini, P., Brown, S.C., Torelli, S., Benson, M.A., Herrmann, R., Anderson, L.V., Bashir, R., Burgunder, J.M., et al. (2001). Mutations in the fukutin-related protein gene (FKRP) identify limb girdle muscular dystrophy 2I as a milder allelic variant of congenital muscular dystrophy MDC1C. Hum. Mol. Genet. *10*, 2851–2859.
14. Martin, P.T. (2007). Congenital muscular dystrophies involving the O-mannose pathway. Curr. Mol. Med. *7*, 417–425.
15. Chan, Y.M., Keramaris-Vrantsis, E., Lidov, H.G., Norton, J.H., Zinchenko, N., Gruber, H.E., Thresher, R., Blake, D.J., Ashar, J., Rosenfeld, J., and Lu, Q.L. (2010). Fukutin-related protein is essential for mouse muscle, brain and eye development and mutation recapitulates the wide clinical spectrums of dystroglycanopathies. Hum. Mol. Genet. *19*, 3995–4006.
16. Kanagawa, M., Kobayashi, K., Tajiri, M., Manya, H., Kuga, A., Yamaguchi, Y., Akasaka-Manya, K., Furukawa, J.I., Mizuno, M., Kawakami, H., et al. (2016). Identification of a post-translational modification with ribitol-phosphate and its defect in muscular dystrophy. Cell Rep. *14*, 2209–2223.
17. Gerin, I., Ury, B., Breloy, I., Bouchet-Seraphin, C., Bolsée, J., Halbout, M., Graff, J., Vertommen, D., Muccioli, G.G., Seta, N., et al. (2016). ISPD produces CDP-ribitol used by FKTN and FKRP to transfer ribitol phosphate onto α-dystroglycan. Nat. Commun. *7*, 11534.
18. Riemersma, M., Froese, D.S., van Tol, W., Engelke, U.F., Kopec, J., van Scherpenzeel, M., Ashikov, A., Krojer, T., von Delft, F., Tessari, M., et al. (2015). Human ISPD is a cytidyltransferase required for dystroglycan O-mannosylation. Chem. Biol. *22*, 1643–1652.
19. Manya, H., Yamaguchi, Y., Kanagawa, M., Kobayashi, K., Tajiri, M., Akasaka-Manya, K., Kawakami, H., Mizuno, M., Wada, Y., Toda, T., and Endo, T. (2016). The muscular dystrophy gene TMEM5 encodes a ribitol β1,4-xylosyltransferase required for the functional glycosylation of dystroglycan. J. Biol. Chem. *291*, 24618–24627.
20. Willer, T., Inamori, K., Venzke, D., Harvey, C., Morgensen, G., Hara, Y., Beltrán Valero de Bernabé, D., Yu, L., Wright, K.M., and Campbell, K.P. (2014). The glucuronyltransferase B4GAT1 is required for initiation of LARGE-mediated α-dystroglycan functional glycosylation. eLife *3*, e03941.
21. Praissman, J.L., Live, D.H., Wang, S., Ramiah, A., Chinoy, Z.S., Boons, G.J., Moremen, K.W., and Wells, L. (2014). B4GAT1 is the priming enzyme for the LARGE-dependent functional glycosylation of α-dystroglycan. eLife *3*, e03943.
22. Briggs, D.C., Yoshida-Moriguchi, T., Zheng, T., Venzke, D., Anderson, M.E., Strazzulli, A., Moracci, M., Yu, L., Hohenester, E., and Campbell, K.P. (2016). Structural basis of laminin binding to the LARGE glycans on dystroglycan. Nat. Chem. Biol. *12*, 810–814.
23. Van Reeuwijk, J., Olderode-Berends, M.J., Van den Elzen, C., Brouwer, O.F., Roscioli, T., Van Pampus, M.G., Scheffer, H., Brunner, H.G., Van Bokhoven, H., and Hol, F.A. (2010). A homozygous FKRP start codon mutation is associated with Walker-Warburg syndrome, the severe end of the clinical spectrum. Clin. Genet. *78*, 275–281.
24. Brockington, M., Blake, D.J., Prandini, P., Brown, S.C., Torelli, S., Benson, M.A., Ponting, C.P., Estournet, B., Romero, N.B., Mercuri, E., et al. (2001). Mutations in the fukutin-related protein gene (FKRP) cause a form of congenital muscular

dystrophy with secondary laminin alpha2 deficiency and abnormal glycosylation of alpha-dystroglycan. Am. J. Hum. Genet. *69*, 1198–1209.

25. Mercuri, E., Brockington, M., Straub, V., Quijano-Roy, S., Yuva, Y., Herrmann, R., Brown, S.C., Torelli, S., Dubowitz, V., Blake, D.J., et al. (2003). Phenotypic spectrum associated with mutations in the fukutin-related protein gene. Ann. Neurol. *53*, 537–542.

26. Mercuri, E., Topaloglu, H., Brockington, M., Berardinelli, A., Pichiecchio, A., Santorelli, F., Rutherford, M., Talim, B., Ricci, E., Voit, T., and Muntoni, F. (2006). Spectrum of brain changes in patients with congenital muscular dystrophy and FKRP gene mutations. Arch. Neurol. *63*, 251–257.

27. Xu, L., Lu, P.J., Wang, C.H., Keramaris, E., Qiao, C., Xiao, B., Blake, D.J., Xiao, X., and Lu, Q.L. (2013). Adeno-associated virus 9 mediated FKRP gene therapy restores functional glycosylation of α-dystroglycan and improves muscle functions. Mol. Ther. *21*, 1832–1840.

28. Qiao, C., Wang, C.H., Zhao, C., Lu, P., Awano, H., Xiao, B., Li, J., Yuan, Z., Dai, Y., Martin, C.B., et al. (2014). Muscle and heart function restoration in a limb girdle muscular dystrophy 2I (LGMD2I) mouse model by systemic FKRP gene delivery. Mol. Ther. *22*, 1890–1899.

29. Vannoy, C.H., Xu, L., Keramaris, E., Lu, P., Xiao, X., and Lu, Q.L. (2014). Adeno-associated virus-mediated overexpression of LARGE rescues α-dystroglycan function in dystrophic mice with mutations in the fukutin-related protein. Hum. Gene Ther. Methods *25*, 187–196.

30. Blaeser, A., Keramaris, E., Chan, Y.M., Sparks, S., Cowley, D., Xiao, X., and Lu, Q.L. (2013). Mouse models of fukutin-related protein mutations show a wide range of disease phenotypes. Hum. Genet. *132*, 923–934.

31. Krag, T.O., Hauerslev, S., Sveen, M.L., Schwartz, M., and Vissing, J. (2011). Level of muscle regeneration in limb-girdle muscular dystrophy type 2I relates to genotype and clinical severity. Skelet. Muscle *1*, 31.

32. Cohn, R.D., Henry, M.D., Michele, D.E., Barresi, R., Saito, F., Moore, S.A., Flanagan, J.D., Skwarchuk, M.W., Robbins, M.E., Mendell, J.R., et al. (2002). Disruption of DAG1 in differentiated skeletal muscle reveals a role for dystroglycan in muscle regeneration. Cell *110*, 639–648.

33. Awano, H., Blaeser, A., Keramaris, E., Xu, L., Tucker, J., Wu, B., Lu, P., and Lu, Q.L. (2015). Restoration of functional glycosylation of α-dystroglycan in FKRP mutant mice is associated with muscle regeneration. Am. J. Pathol. *185*, 2025–2037.

34. Keramaris, E., Lu, P.J., Tucker, J., and Lu, Q.L. (2017). Expression of glycosylated α-dystroglycan in newborn skeletal and cardiac muscles of fukutin related protein (*FKRP*) mutant mice. Muscle Nerve *55*, 582–590.

35. Keramaris-Vrantsis, E., Lu, P.J., Doran, T., Zillmer, A., Ashar, J., Esapa, C.T., Benson, M.A., Blake, D.J., Rosenfeld, J., and Lu, Q.L. (2007). Fukutin-related protein localizes to the Golgi apparatus and mutations lead to mislocalization in muscle in vivo. Muscle Nerve *36*, 455–465.

36. Esapa, C.T., McIlhinney, R.A., and Blake, D.J. (2005). Fukutin-related protein mutations that cause congenital muscular dystrophy result in ER-retention of the mutant protein in cultured cells. Hum. Mol. Genet. *14*, 295–305.

37. Esapa, C.T., Benson, M.A., Schröder, J.E., Martin-Rendon, E., Brockington, M., Brown, S.C., Muntoni, F., Kröger, S., and Blake, D.J. (2002). Functional requirements for fukutin-related protein in the Golgi apparatus. Hum. Mol. Genet. *11*, 3319–3331.

38. Vannoy, C.H., Xiao, W., Lu, P., Xiao, X., and Lu, Q.L. (2017). Efficacy of gene therapy is dependent on disease progression in dystrophic mice with mutations in the FKRP gene. Mol. Ther. Methods Clin. Dev. *5*, 31–42.

39. Hsu, C.C., Li, H.P., Hung, Y.H., Leu, Y.W., Wu, W.H., Wang, F.S., Lee, K.D., Chang, P.J., Wu, C.S., Lu, Y.J., et al. (2010). Targeted methylation of CMV and E1A viral promoters. Biochem. Biophys. Res. Commun. *402*, 228–234.

40. Koeberl, D.D., Sun, B.D., Damodaran, T.V., Brown, T., Millington, D.S., Benjamin, D.K., Jr., Bird, A., Schneider, A., Hillman, S., Jackson, M., et al. (2006). Early, sustained efficacy of adeno-associated virus vector-mediated gene therapy in glycogen storage disease type Ia. Gene Ther. *13*, 1281–1289.

41. Ferrer, A., Wells, K.E., and Wells, D.J. (2000). Immune responses to dystropin: implications for gene therapy of Duchenne muscular dystrophy. Gene Ther. *7*, 1439–1446.

42. England, S.B., Nicholson, L.V., Johnson, M.A., Forrest, S.M., Love, D.R., Zubrzycka-Gaarn, E.E., Bulman, D.E., Harris, J.B., and Davies, K.E. (1990). Very mild muscular dystrophy associated with the deletion of 46% of dystrophin. Nature *343*, 180–182.

43. Mendell, J.R., Campbell, K., Rodino-Klapac, L., Sahenk, Z., Shilling, C., Lewis, S., Bowles, D., Gray, S., Li, C., Galloway, G., et al. (2010). Dystrophin immunity in Duchenne's muscular dystrophy. N. Engl. J. Med. *363*, 1429–1437.

44. Malik, V., Rodino-Klapac, L.R., Viollet, L., Wall, C., King, W., Al-Dahhak, R., Lewis, S., Shilling, C.J., Kota, J., Serrano-Munuera, C., et al. (2010). Gentamicin-induced readthrough of stop codons in Duchenne muscular dystrophy. Ann. Neurol. *67*, 771–780.

45. Antun, A., Monahan, P.E., Manco-Johnson, M.J., Callaghan, M.U., Kanin, M., Knoll, C., Carpenter, S.L., Davis, J.A., Guerrera, M.F., Kruse-Jarres, R., et al. (2015). Inhibitor recurrence after immune tolerance induction: a multicenter retrospective cohort study. J. Thromb. Haemost. *13*, 1980–1988.

46. Gicquel, E., Maizonnier, N., Foltz, S.J., Martin, W.J., Bourg, N., Svinartchouk, F., Charton, K., Beedle, A.M., and Richard, I. (2017). AAV-mediated transfer of FKRP shows therapeutic efficacy in a murine model but requires control of gene expression. Hum. Mol. Genet. *26*, 1952–1965.

47. Rasband, W.S. (1997) ImageJ (NIH, Bethesda, MD, USA). https://imagej.nih.gov/ij/.

OMTN, Volume *11*

Supplemental Information

Overexpression of Mutant FKRP Restores Functional Glycosylation and Improves Dystrophic Phenotype in FKRP Mutant Mice

Jason D. Tucker, Pei J. Lu, Xiao Xiao, and Qi L. Lu

SUPPLEMENTAL INFORMATION

Overexpression of Mutant FKRP Associated with CMD Restores Functional Glycosylation and Improves Dystrophic Phenotype in Skeletal and Cardiac Muscle of FKRP mutant Mice

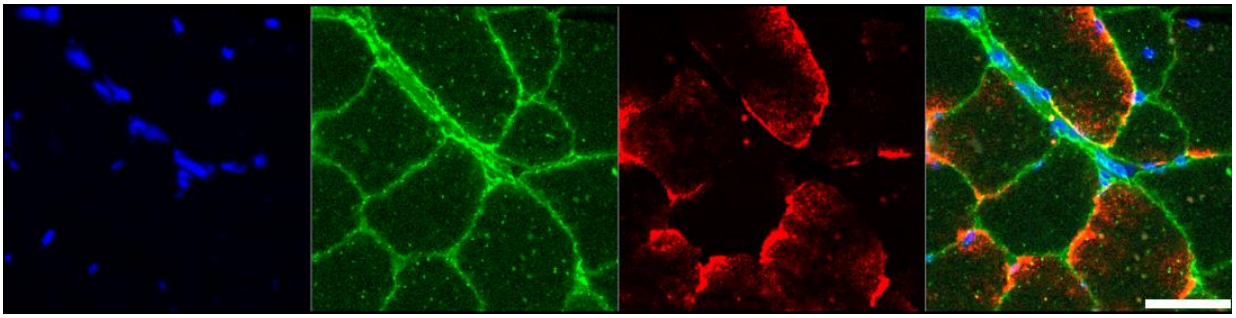

SI Figure 1. Localization of GM130 (green as a Golgi marker presenting as points within the cytoplasm and along fiber membrane) and mhFKRP (red) in *P448Lneo*$^{-}$ TA muscles 1 month after AAV9-*mhFKRP* 5e13 vg/kg treatment by confocal microscopy. No consistent co-localization of the two signals was observed. Scale Bars = 50 µm

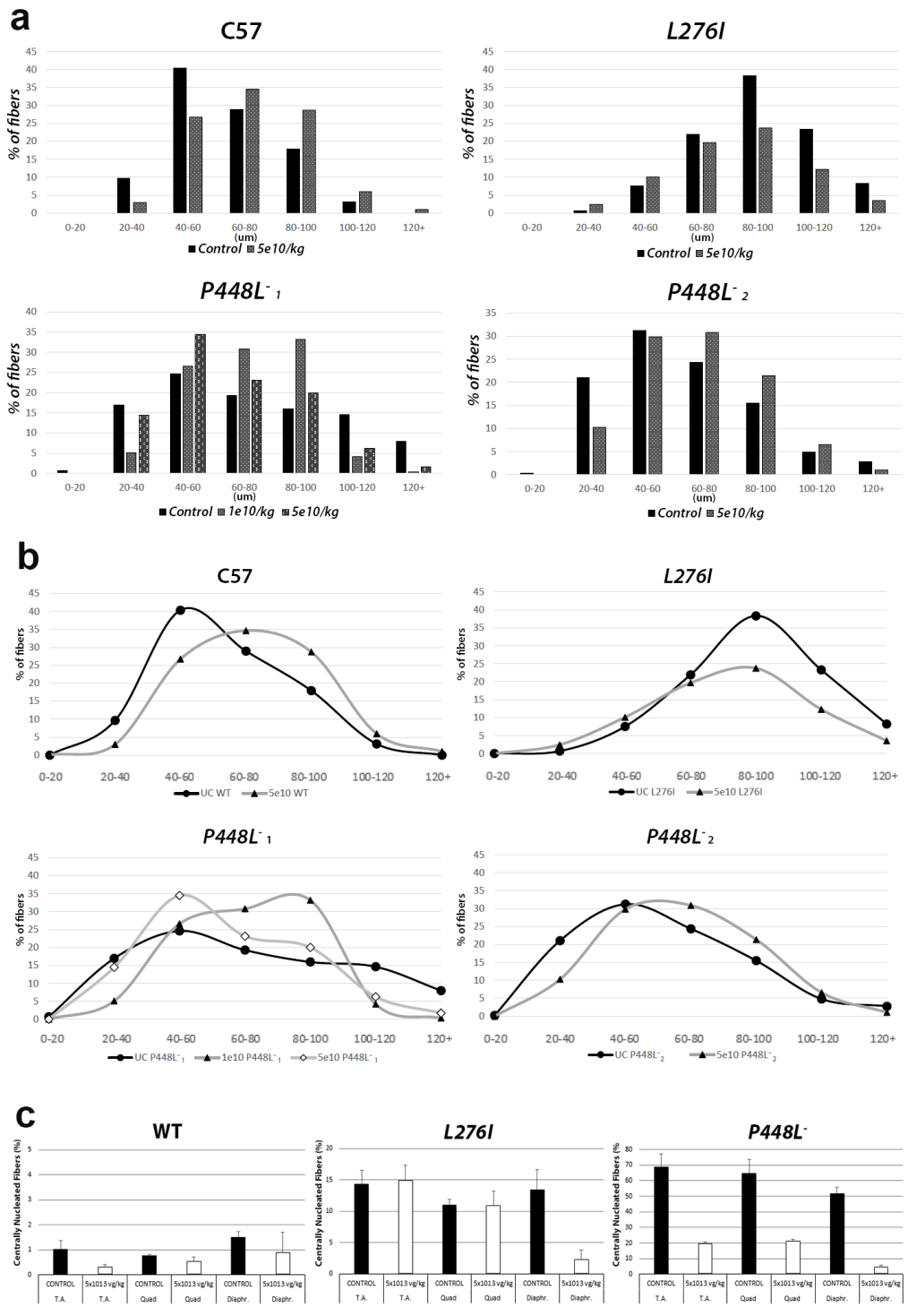

SI Figure 2. (A) Morphometric distribution of skeletal muscle fiber diameters (μm) in treated and control *C57BL/6*, *L276I* and *FKRP* mutant mice one month after AAV9-*mhFKRP* administration. **(B)** Line representation of the same data, more clearly demonstrating shifts in distribution patterns. **(C)** Centrally nucleated fibers of the TA, quadriceps, and diaphragm of control and treated *C57BL/6*, *P448L*$^{-}$ and *L276I* mutant mice after one-month treatment with AAV9-*mhFKRP*. Error bars represent the standard error of the mean (SEM).

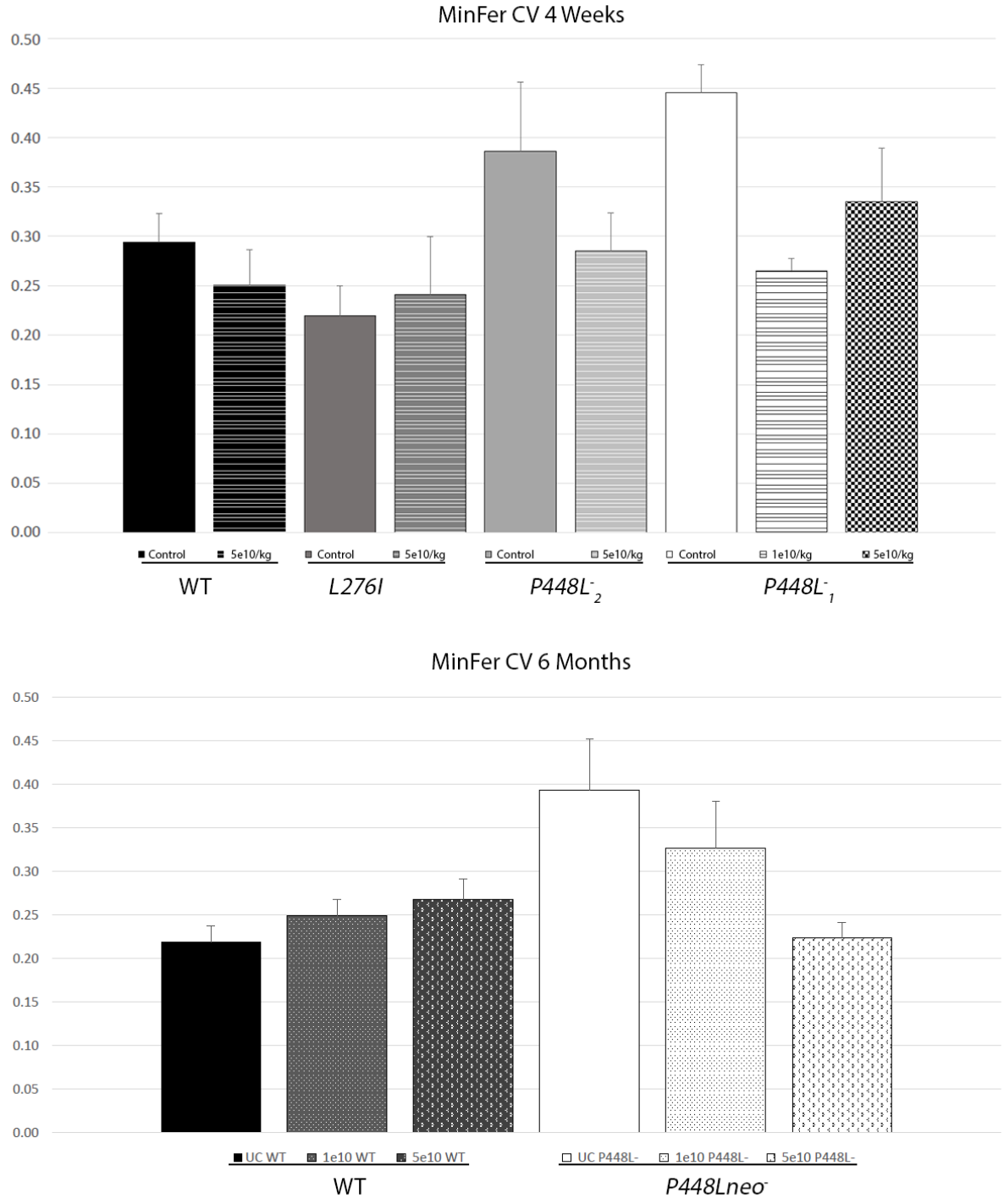

SI Figure 3. Coefficient of variance (CV) calculated from morphometric measures 'MinFer' (ImageJ) in *C57BL/6* (WT) and *FKRP* mutant mice one month after AAV9-*mhFKRP* treatment. Reduction in the CV, indicating a more homogenous muscle fiber composition can be observed as early as one month after AAV9-*mhFKRP* administration in all treated groups, with the exception of the WT and *L276I* groups which were relatively unchanged. At six months, both 1e13 vg/kg and 5e13 vg/kg treated *P448Lneo*$^{-}$ cohorts demonstrated reduced CV in fiber sizes with variance more closely resembling WT.